Journal of Structural Geology, Vol. 7, Nos. 3/4, pp. 385 to 400, 1985
Printed in Great Britain

0191-8141/85 $03.00 + 0.00
Pergamon Press Ltd.

Significance of the early foliation at Bermagui, N.S.W., Australia

C. McA. Powell

Australian Plate Research Group, School of Earth Sciences, Macquarie University, North Ryde, N.S.W. 2113, Australia

and

M. J. Rickard

Department of Geology, Australian National University, Canberra, A.C.T. 2601, Australia

(*Received* 9 *February* 1984; *accepted in revised form* 3 *July* 1984)

Abstract—The first-generation mesoscopic folds, F_1, in the Ordovician turbidites at Bermagui, N.S.W., Australia, are tight to locally isoclinal and have a convergently fanning axial-surface foliation, S_1, which is a differentiated crenulation cleavage. S_1 overprints an earlier foliation, herein called S^*. In psammites, S^* is a strong alignment of mineral grains and rough, micaceous folia, and in pelites S^* is a microbanding of quartzose and micaceous layers. Depending on rock type and position in the F_1 fold profile, S^* may be (1) parallel to bedding, (2) rotated out of parallelism with bedding by the S_1 cleavage and (3) truly cross-cutting bedding. In many places, S^* cuts across bedding demonstrating that it is a superimposed tectonic foliation and not simply an inherited depositional fabric. In outcrops south of Bermagui, S^* changes vergence with apparent congruence with F_1 folds. In other outcrops near Bermagui, however, S^* maintains a constant vergence around F_1 folds, the geometry indicating a pre-F_1 anticline to the east. Since there is no evidence for large-scale pre-F_1 folds, the various relations of S^* *to* S_1 and F_1 are best explained by the rarely described process of late-stage hinge nucleation during a single protracted F_1 folding sequence. Other possibilities such as fold-hinge migration and pre-fold imbricate stacking are discussed but considered less likely.

INTRODUCTION

Deformed quartzose turbidites, probably of Ordovician age, are exposed along the New South Wales south coast and in adjacent eastern Victoria. Structural analysis of small areas has delineated two main generations of folding (Hobbs 1962, Wilson 1968, Williams 1971, Cole 1982, Wilson *et al.* 1982), although Powell (1983a) described three phases of mesoscopic folding in the Bermagui region. The first generation of folding in each of these studies is the same, and where not rotated by later folding, is generally upright and N–S trending, with close to nearly isoclinal fold profiles and a well-developed convergently fanning axial-surface cleavage. In a series of well-known papers on the Bermagui area, Williams (1970, 1971, 1972) described the cleavage related to this first generation of mesoscopic folds as a differentiated crenulation cleavage which, in appropriate pelitic rock types, is sufficiently closely spaced to appear slaty in outcrop. In some pelites the sedimentary lamination gives a crenulation morphology to S_1 (e.g. Williams 1979). In medium- to coarse-grained graded beds, this first-generation axial-surface cleavage may appear as bands of pelitic material, spaced centimetres apart, giving the rocks a stripy appearance in outcrop (e.g. Williams 1982).

The crenulation morphology of the cleavage parallel to the axial surface of the first generation of mesoscopic folds is caused by the presence of an early foliation. In many places, this early foliation is a strong grain alignment with dark, anastomosing, pelitic folia wrapping around modified detrital grains. The morphology of the early fabric in psammites is that of a rough cleavage (Gray 1978, 1982), with mica beards accentuating the grain alignment. In pelites, the early fabric is a smooth fine banding of alternating quartzose and micaceous layers. Williams (1972, p. 35) considered that this early fabric was either detrital in origin, or a later structure inheriting a depositional orientation. He recognized the possibility that the early fabric might have been modified by later diagenetic and low-grade metamorphic processes, but regarded these as secondary effects superimposed on a primarily depositional orientation. Following this explanation, we expected that the early fabric would be parallel to bedding everywhere, and would be cut by any post-depositional structures. On the contrary, we found many places where the early fabric is not only oblique to bedding, but also cuts across quartz veins formed after the rocks were consolidated. This raises the possibility of a pre-F_1 deformation, previously unrecognized.

The significance of these observations is that they imply either that the crenulation cleavage is a transecting foliation or that there was an earlier folding and cleavage-producing event. However, transection does not occur and no early folds were found. Moreover, the vergence relations support the postulate that the two cleavages may be related to a single set of folds. An additional complication is that many F_1 folds are so tight that both cleavages (S^* and S_1) are virtually parallel to S_0 on some fold limbs, thus enhancing the appearance of bedding-parallel foliation.

STRUCTURAL DESCRIPTION

Nomenclature

We follow the convention of labelling bedding, S_0, and the first recognisable generation of folds, F_1, with the axial surface as S_1. This makes our F_1 and S_1 the same as Williams' (1970, 1971) B_1 and S_1, although subsequently Williams (1972) used morphological parameters to refine his classification of surfaces designated S_1. The early foliation, which is not always parallel to bedding, thus poses a nomenclatural problem because in places it is oblique to, and younger than S_0, but older than S_1. Powell (1983a) attempted to resolve this dilemma by referring to the early fabric as $S_{1/2}$ thus maintaining the identity of later cleavage subscript numbers with those of the folds to which they are related. However, because a possible explanation for some of the relationships observed involves formation of the early foliation during F_1 with subsequent fold-hinge migration or later-stage hinge nucleation, we use the symbol S^* to refer to the earlier foliation cut by the axial-surface differentiated cleavage, S_1. We thus leave open the question of whether S^* was formed during F_1, during an earlier deformation or was partially inherited from depositional processes.

Places where S is oblique to S_0*

In the field, there appear to be many places where S^* lies oblique to S_0, and is cut by S_1. This is especially so in thicker psammite beds where, within a bed, there may be a strong grain orientation markedly oblique to both S_0 and S_1. However, when the grain orientation is traced carefully into a contact between two beds of contrasting grain size or composition, S^* in many places is seen to curve into parallelism with S_0. The apparently oblique relationship within the bed is thus not maintained everywhere at the bedding contact. This 'optical-illusion' effect (discussed more fully later) means that the only place where an unequivocal time relationship between S^* and S_0 can be established is where S^* can be traced out of one bed into another. Moreover, because the grain size is commonly too fine to be seen with the unaided eye, we have found it necessary to use large thin-sections that span psammite–pelite contacts. We have restricted our work to areas where the local structure is well documented, so that there is no confusion about which generation of folds or which S-surface is being considered. Because establishment of the relationship of S^* to S_0 and S_1 is the crux of our argument, we have relied mainly on photographic documentation, and kept description to bare essentials.

There are two easily accessible areas where S^* lies oblique to S_0 and is cut by S_1, and reconnaisance shows that similar relationships exist in several other places.

Area 1—Bermagui Headland GR 376650 Bermagui

The Bermagui Headland area (Fig. 1a) is a relatively simply deformed area for which a map (Williams 1970, fig. 7b) and a partial cross-section (Powell 1983a, fig. 52) have been published. Regionally, the area lies on the western limb of a W-facing F_1 anticline, so that most of the bedding and folds young westward (Fig. 1b). The western limbs of mesoscopic anticlines are steep, and locally overturned, with generally moderate dips on the E-dipping upright, eastern limbs. Faults quasi-parallel to the fold axial surfaces disrupt the section, but do not affect the overall W-verging symmetry. All the large mesoscopic folds are F_1, and the axial-surface crenulation cleavage, S_1, dips east at approximately 54° (Powell 1983a, fig. 52). There are later cross-cutting crenulation cleavages in the outcrop, but these are very minor and do not affect many parts of the rock.

Oriented specimens were collected at several points along the wave-cut platform (Specimens BH1 to 6, Fig. 1). The field appearance of S^* oblique to both S_0 and S_1 is shown in Fig. 2. Figure 2(a) shows the lower part of a psammite bed and the adjacent pelite. S_0 is a well-defined contact that stands out in weathered profile. S_1 in the psammite is a 0.5–1 cm-spaced differentiated crenulation cleavage, pelitic domains providing the surfaces along which the rock tends to split. In the psammite bed, S^* is a strong grain orientation lying in the acute angle between S_0 and S_1. S^* makes a lower angle with S_1 in the pelitic (dark) domains than in the lighter-coloured leucocratic zones. In the pelite bed, S^* refracts to a nearly vertical orientation, and becomes a very finely banded foliation. S_1 is more closely spaced in the pelite than in the psammite, with planar, discrete traces apparent just west of the 20 cent coin.

The broad-scale thin-section view of a psammite–pelite bedding contact is shown in Fig. 3(a). S_1 is defined by bundles of dark pelitic folia, which produce a step where they cross the bedding contact. In the psammite a grain-alignment fabric is rotated as it passes through the S_1 cleavage domains, and appears to be approximately parallel to the psammite–pelite bedding contact close to the base of the bed. A weak wispy fabric lying in the acute angle between S_0 and S_1 represents S^*. The discrete S_1 domains in the psammite can be traced across the S_0 contact into the pelite where they are more uniformly distributed through the rock. Close inspection of Fig. 3(a) shows that S_1 cuts very fine alternating light and dark bands (S^*) in the pelite, and that this fine banding runs obliquely into the bedding contact between the psammite and pelite. Moreover, quartz veins parallel to this fine banding are folded by S_1.

An enlarged view of the eastern part of Fig. 3(a) shows that here the fine banding in the pelite is a series of very thin quartz veins, which have been folded into sub-millimetre wavelength isoclinal folds with S^* parallel to their axial surfaces (Fig. 3b, upper centre part). The hinges of many of these isoclinal folds have been truncated by solution-removal along S_1 surfaces, but closures are still preserved in places.

Another example of S^* lying oblique to S_0 and, in turn, being cut by S_1 is also shown in Fig. 4, located on the near-vertical eastern limb of a syncline. In this

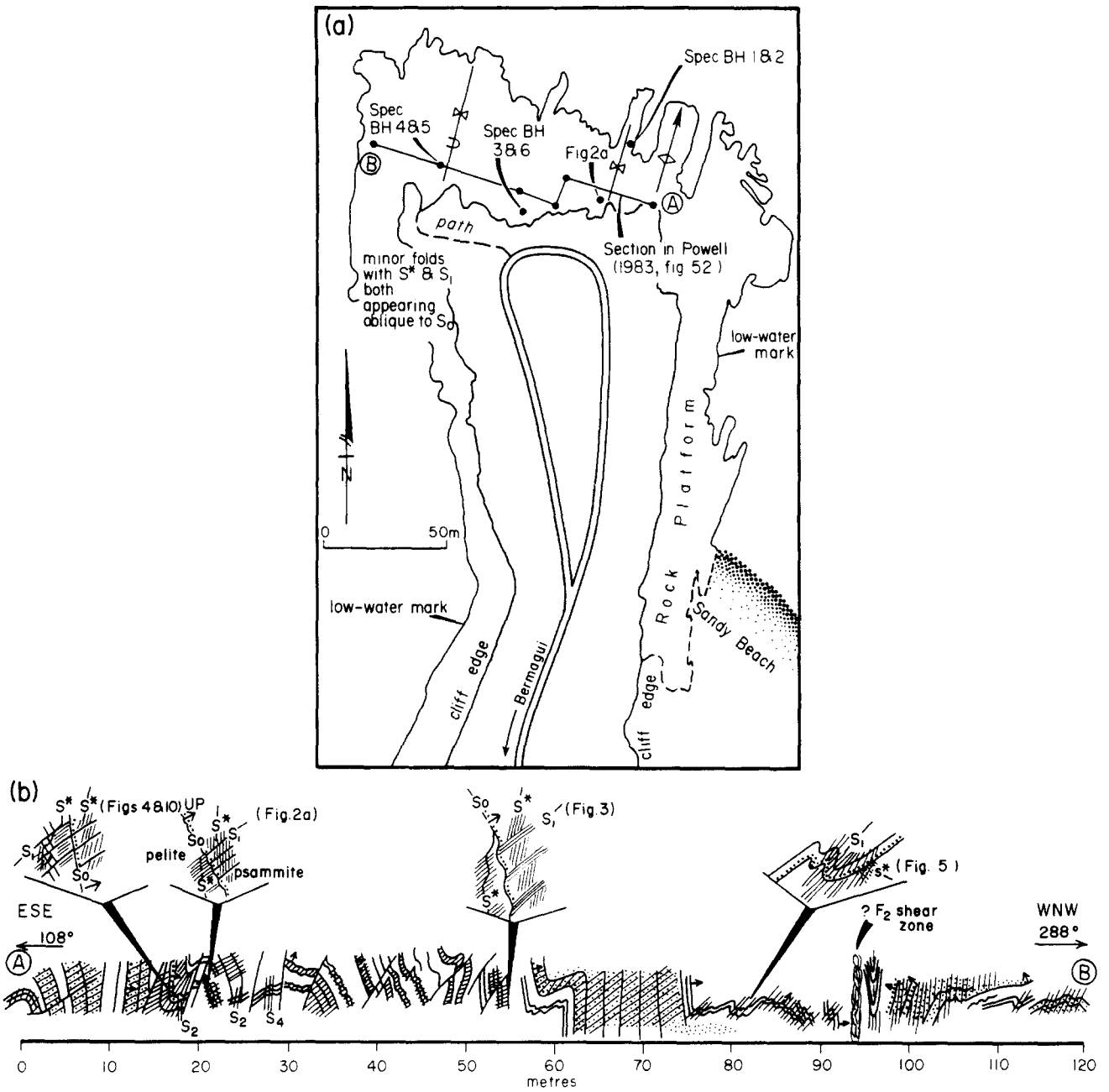

Fig. 1. (a) Map of the Bermagui Headland area, with location of figured specimens indicated. Outline traced from an enlarged aerial photograph. (b) Structural profile A–B located in (a). Location of figured material indicated in exploded views. The entire profile lies on the steep western limb of a W-facing inclined F_1 anticline.

structural position, S_1 makes a relatively high angle with S_0, and the obliquity of S^* to S_0 can be seen where S^* intersects a thin siltstone layer partially disrupted by dissolution on S_1. The intensely penetrative, finely banded nature of S^* in the pelite is seen best in the enlarged view (Fig. 4b). In the silty band, discontinuous wavy cleavage traces at a higher angle to S_0 than in the pelite, probably represent S^*. These fine, anastomosing cleavage traces are sharply truncated by the dark S_1 cleavage bundles. In the psammite, S^* appears as a rough cleavage elongate approximately parallel to S_0, and two very elongate shale clasts (length : width ratio 20 : 1) are aligned in it. S_1 crenulates S^* in these pelite clasts.

Figure 5 shows a thin-section taken from the more gently dipping western limb of a syncline at the western end of the headland outcrop. In this position, S_0 dips moderately, and S_1 steeply, to the east. S^* in the pelite dips westward, almost at right angles to the bedding, but in the psammite S^* is subparallel to S_0. In the lower left-hand part of the broad view (Fig. 5a), S_0, S^* and S_1 can be seen as three distinct surfaces, S^* appearing as a discontinuous, wavy cleavage in the light-coloured siltstone, and as a fine banding in the pelite. S_1 appears as discrete crenulation–cleavage surfaces, commonly offsetting quartz veins by dissolution.

The enlarged view in Fig. 5(b) shows the nature of S_0, S^* and S_1 in the upper left-hand part of Fig. 5(a). Quartz veins can be traced out of the pelite and across the bedding contact into the psammite where S^* is nearly parallel to S_0. At the margins of the quartz vein in the centre upper part of Fig. 5(b), and also just to the left

(west) of it, fibrous quartz intergrowths parallel to S^* in the psammite indicate dissolution and precipitation of quartz during the development of S^*. The steeper angle S^* makes with S_0 in the pelite compared with the psammite is consistent with layer-parallel shear of an acutely inclined S^* originally verging anticlinally to the east (Fig. 5b), the later shear being in sense congruous with the present position of the specimen on the western limb of the minor syncline (Fig. 5, inset diagram). The sense of this shear is such as to increase greatly the initial small angle between S^* and S_0 in the pelite, while leaving the initial angle in the psammite unchanged.

Area 2—North of Zane Grey Pool

The second area where S^* can be observed oblique to S_0 is on the NE-facing rock platform a few hundred metres north of Zane Grey Pool (Fig. 6a). A map and section through part of this area has been presented by Powell (1983a, fig. 53), and a spectacular F_1 fold from the southeastern part of the area is figured in Williams (1972, plate 1).

The area is structurally more complex than the Bermagui Headland area, with abundant mesoscopic F_1 folds rotated to recumbent attitude by a zone of open, upright F_2 folds (Powell 1983a). Younger F_3 folds trending SSE are superimposed on both earlier fold systems, but F_3 does not significantly modify the attitudes of the F_1 and F_2 folds.

S^* oblique to S_0 can be seen in outcrop (Fig. 2b) in a number of places along the structural profile drawn by Powell (1983a, fig. 53). Specimens for thin-section analysis were collected here and to the north. Specimen ZG2 is of a hand-specimen sized recumbent syncline parasitic on a cascade of recumbent F_1 folds just north of the sandy beach (Fig. 6b). In broad-scale view (Fig. 7a), S_0 and S^* are folded with a relatively weak development of S_1 parallel to the axial surface. On the overturned upper limb (Fig. 7b), there is a strongly developed bedding-parallel grain alignment in the psammite with a weakly developed rough cleavage (S_1) oblique to S_0. The pelite has only one cleavage—a very strongly developed microbanding of quartzose and pelitic layers, which reflects the accumulated effects of S^* and S_1.

The separation of S^* from S_1 becomes obvious only as one traces the banding in the pelite around the fold nose (Fig. 7c). Here, S^* maintains a small angle to S_0 with a constant sense of vergence, whereas S_1 is represented by a younger cross-cutting cleavage of opposite vergence. S_1 changes vergence congruously with its position around the minor fold, whereas S^* maintains a constant vergence, indicating that it pre-dates the fold. When the overturned limb of this hand-specimen sized fold is restored to an upright position, S^* verges anticlinally to the east, and this vergence holds for all other places where S^* is oblique to S_0 and apparently folded by F_1 (e.g. western end of Mill Beach, GR 3617 5680 Bermagui). These examples are all on the western steep limbs of decametric F_1 anticlines (Figs. 1b and 6b).

A portion of the upright limb of a recumbent F_1 fold nearby is shown in Fig. 8. The base of the graded bed at

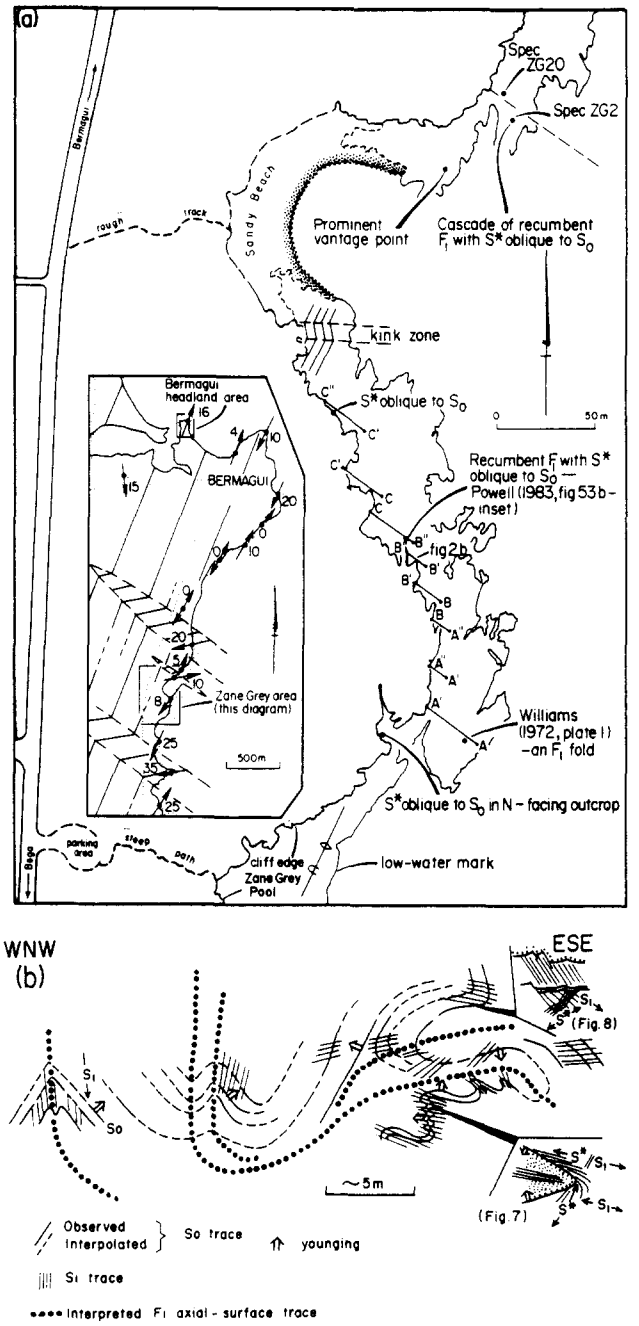

Fig. 6. (a) Location map of the rock-platform outcrops north of Zane Grey Pool. Part of the area is presented as figs. 53a–c in Powell (1983a). Outlines traced from an enlarged aerial photograph. Inset map shows location of the Bermagui Headland and Zane Grey Pool areas on the regional megakink (F_3) map of Powell *et al.* (1985). (b) Structural profile through northern part of the area. Enlargements show location of Figs. 7 and 8.

the top of Fig. 8(a) shows fault-like offsets, and S_1 at a high angle to S_0. In the underlying silty bands, S_1 is expressed as discrete, rough, anastomosing to wavy cleavage surfaces at a high angle to S_0. In the pelitic layer towards the bottom of Fig. 8(a), S_1 is refracted to a lower angle, dipping east, and it crenulates a very fine, penetrative banding, which is S^*. The enlarged view (Fig. 8b) shows more clearly the cross-cutting nature of S_1 on S^*. In the right of Fig. 8(b), a small fold in the light-coloured silty band has S_1 parallel to its axial plane, and deforms S^*. In the field, S^* can be seen to be folded by decimetre-sized recumbent F_1 folds.

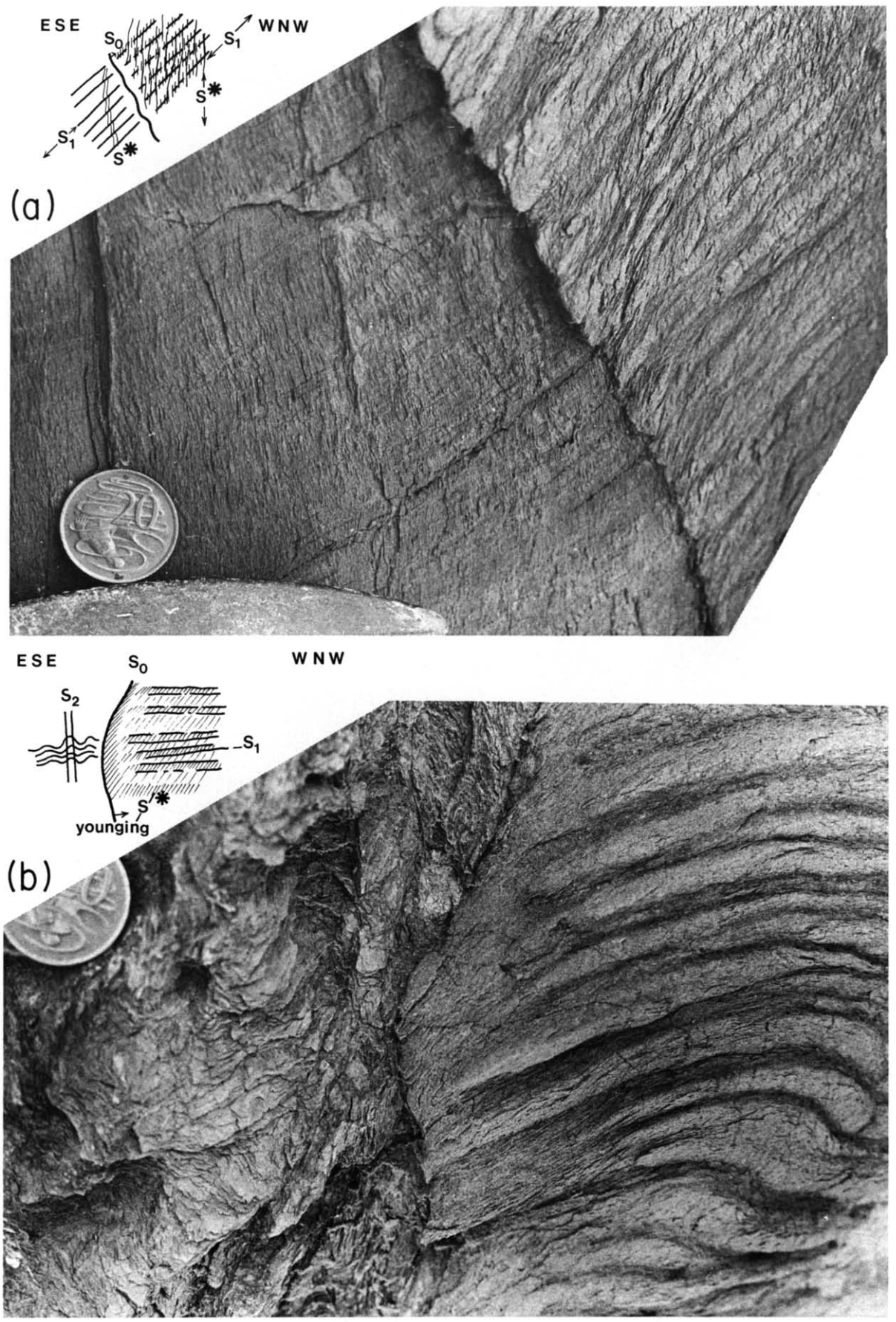

Fig. 2. Outcrop photographs showing S^* oblique to S_0 and S_1. (a) Bermagui Headland, at about 20 m on the profile in Fig. 1(b). (b) North of Zane Grey Pool, near point B′ on the profile in Powell (1983a, fig. 53b). Location is arrowed on Fig. 6(a). The diameter of the 20 cent coin in each photograph is 28 mm.

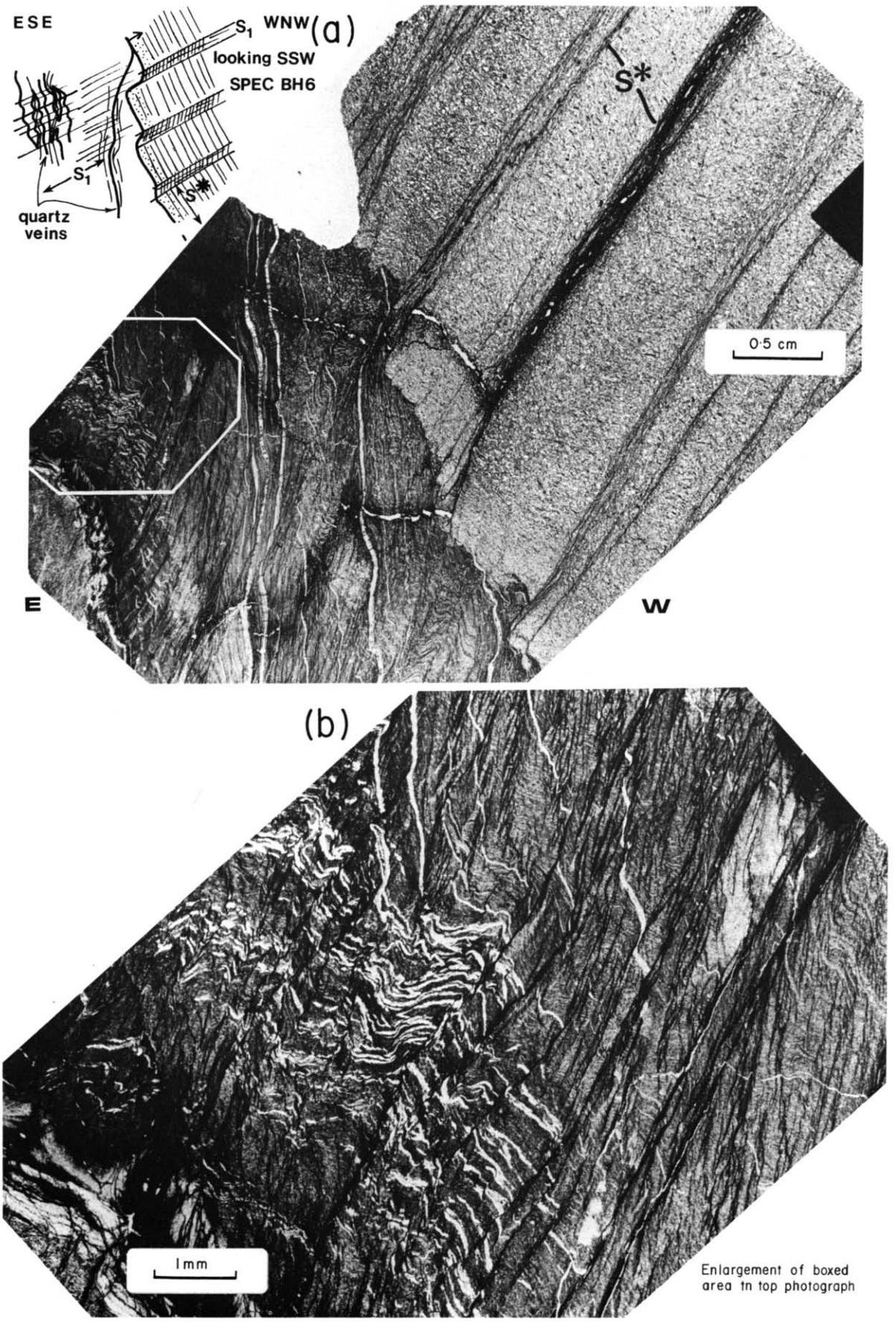

Fig. 3. S_1 cutting S^*, which is oblique to S_0. S_0 dips 78° towards 292°, and S_1 35° towards 115° in the psammite. (a) Broad-scale view of psammite–pelite contact. (b) Detail of inset area showing isoclinal folds in quartz veins with S^* as axial surface. Location: Bermagui Headland, Specimen BH6, about 54 m on the profile in Fig. 1(b).

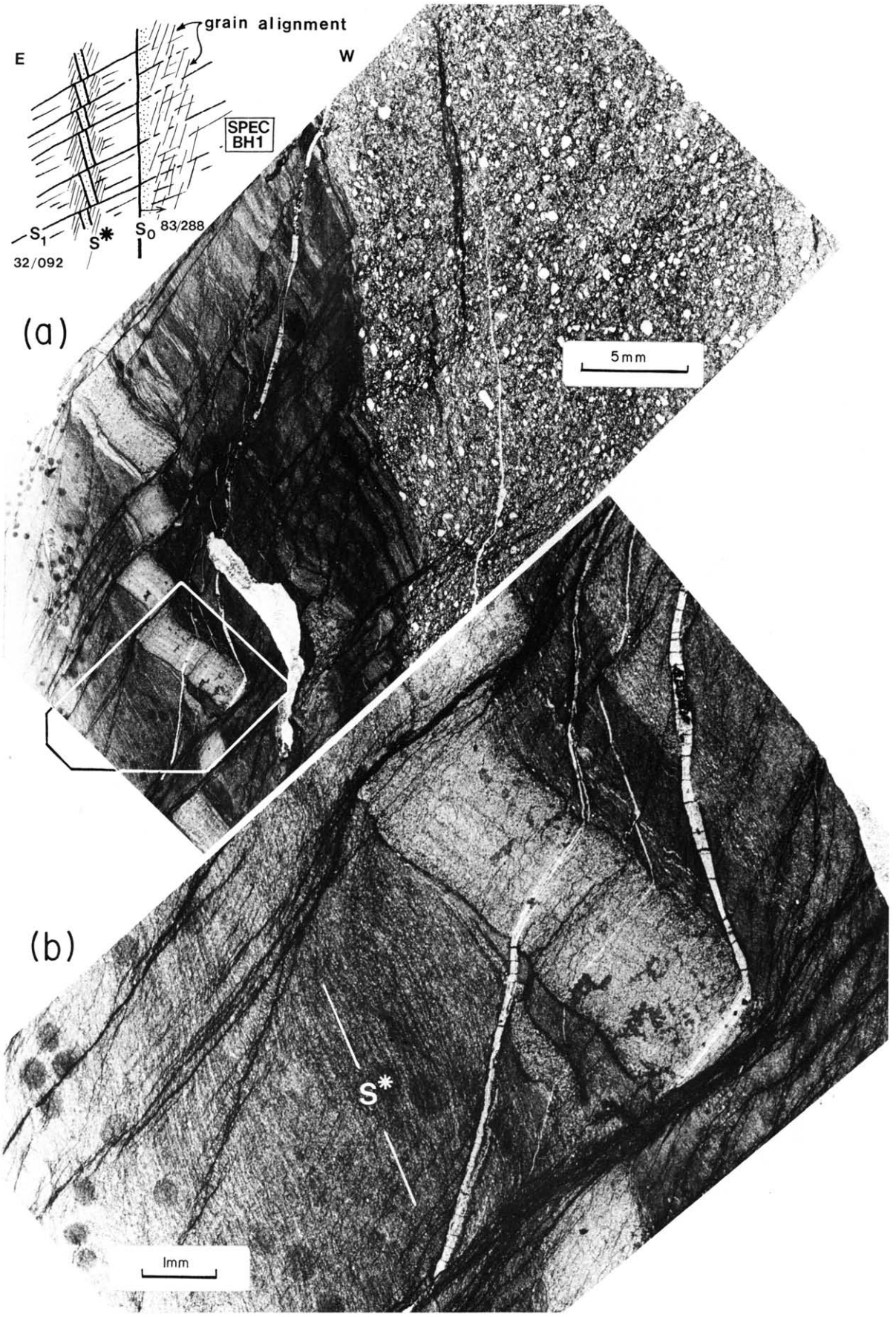

Fig. 4. S^* and S_1 oblique to S_0 on the steep W-facing limb of an F_1 syncline. (a) Broad-scale view. (b) Detail of inset area. Location: Bermagui Headland, Specimen BH1, about 15 m on profile in Fig. 1(b).

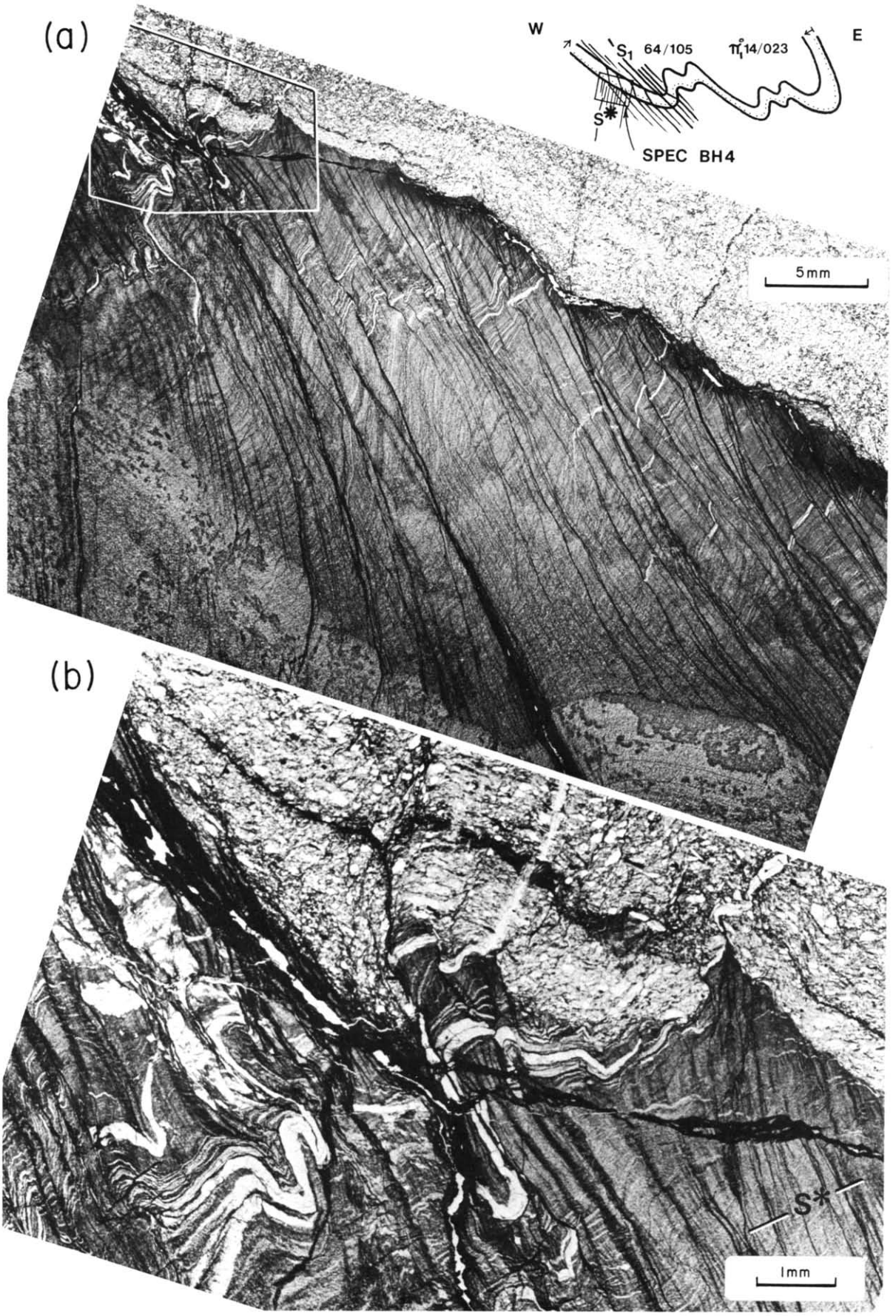

Fig. 5. S^* at a high angle to S_0 on the upright E-dipping limb of a mesoscopic F_1 syncline. (a) Broad-scale view. (b) Detail of inset area. Location: Bermagui Headland, Specimen BH4 at 82 m on profile in Fig. 1(b).

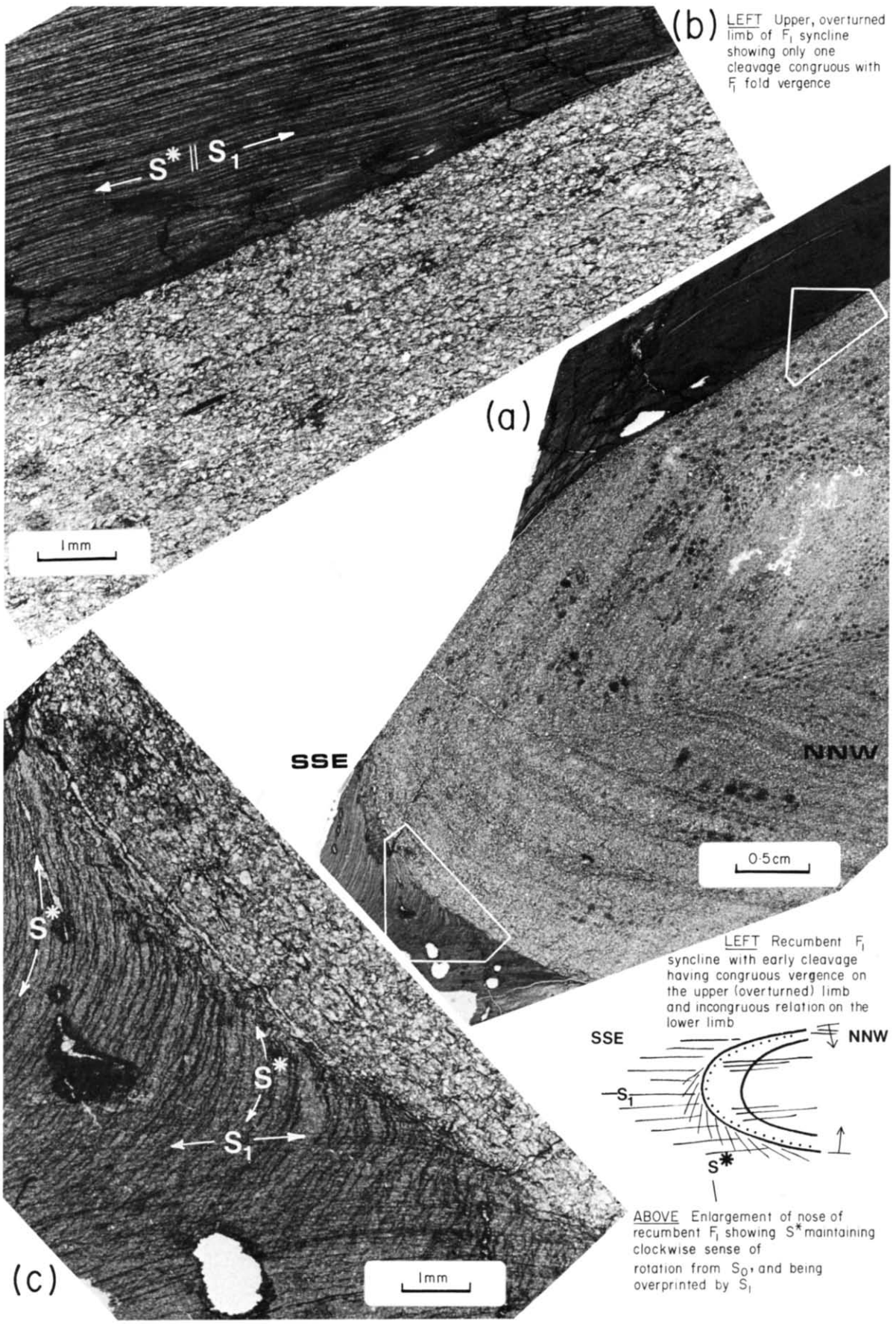

Fig. 7. S^* folded by a recumbent F_1 syncline. (a) Broad-scale view of a thin-section through the recumbent syncline. (b) Detail of the upper, overturned limb. (c) Detail of the nose where S^* maintains its pre-F_1 vergence, and is cut by S_1. Location: Specimen ZG2 from the cascade of recumbent F_1 at GR 376627 Bermagui, north of the first sandy beach north of Zane Grey Pool. Location arrowed in Fig. 6.

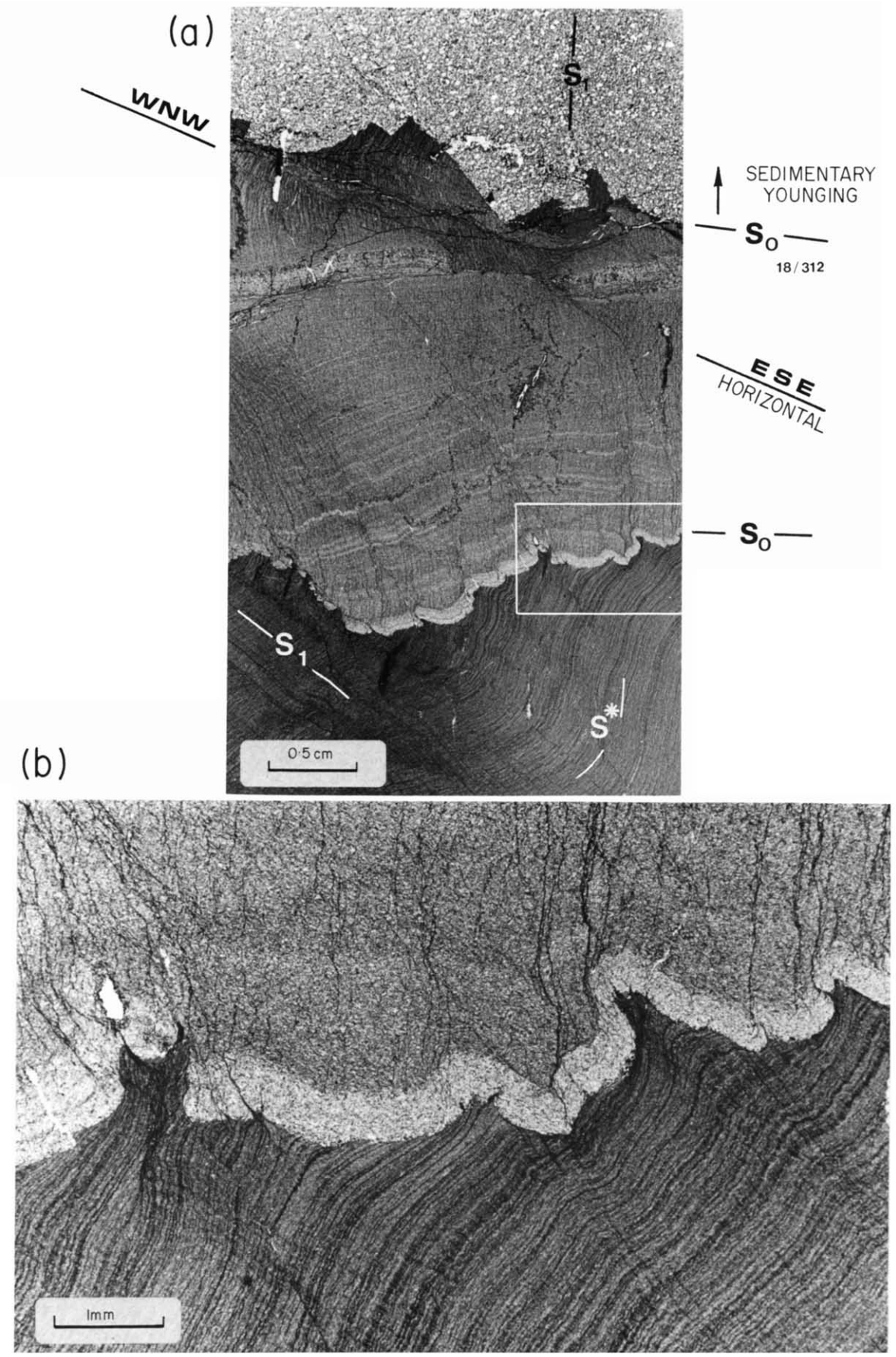

Fig. 8. S^* at a high angle to S_0, with both cut by S_1 on the upright limb of an overturned F_1 fold. S_1 dips 73° towards 118° in the psammite, and S^* in the psammite was measured in outcrop to dip 62° towards 297°. (a) Broad-scale view. (b) Detail of S_0, S^* and S_1 in inset area. Location: Specimen ZG20 from the cascade of folds at GR376627 Bermagui. Location arrowed in Fig. 6.

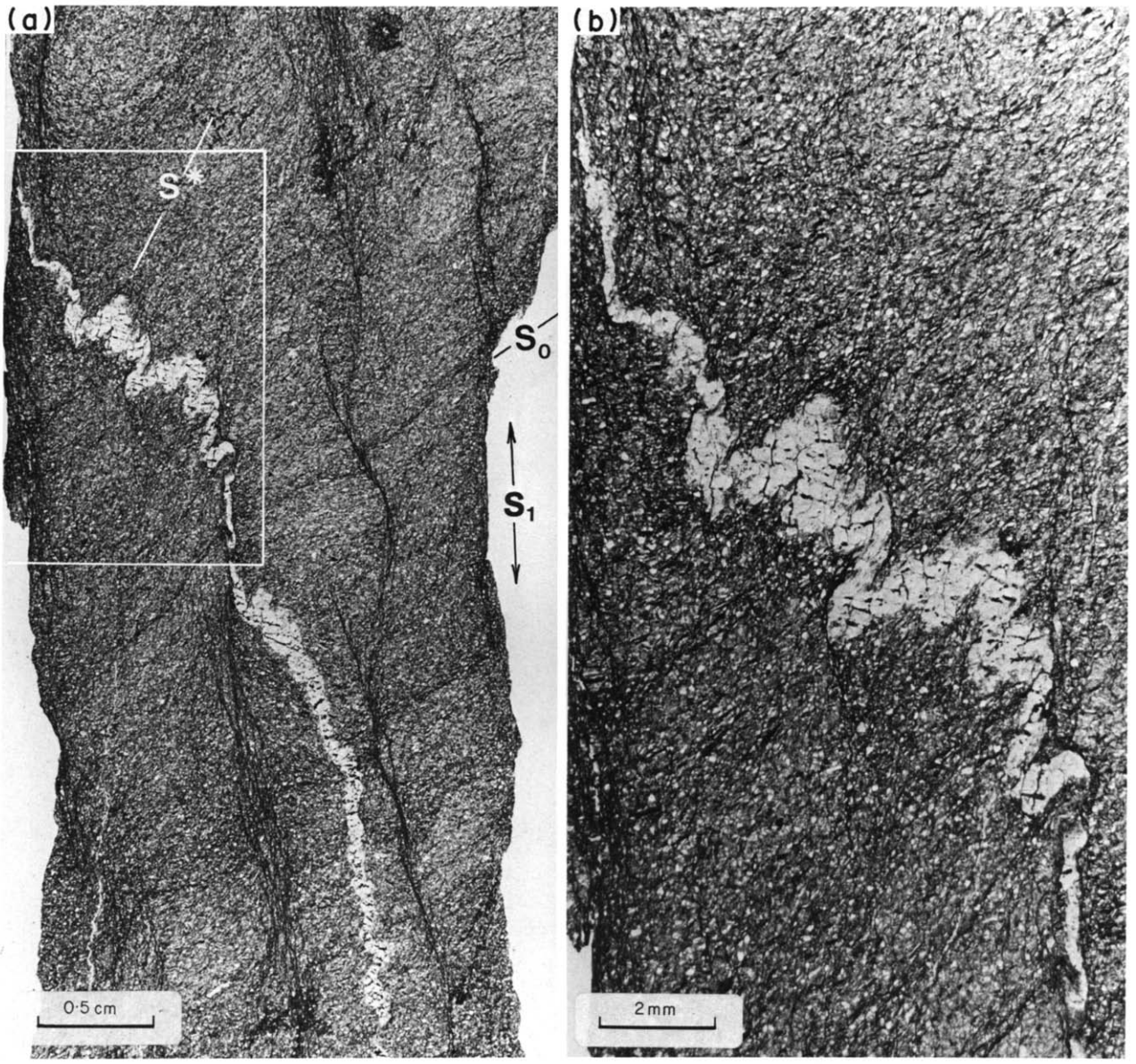

Fig. 9. Small near-isoclinal folds in a quartz vein, with S^* parallel to the axial surface. S_1 is expressed as cm-spaced bundles of dark pelitic folia that thin and locally truncate the quartz vein in a plane oblique to S^*. (a) Broad-scale view. S_0 dips towards the west, and S_1 dips 73° towards 122°. (b) Detail of folds in the quartz vein and the short, rough cleavage traces of S^*. Location: specimen BG2 from Barragga Point (GR 364563 Murrah).

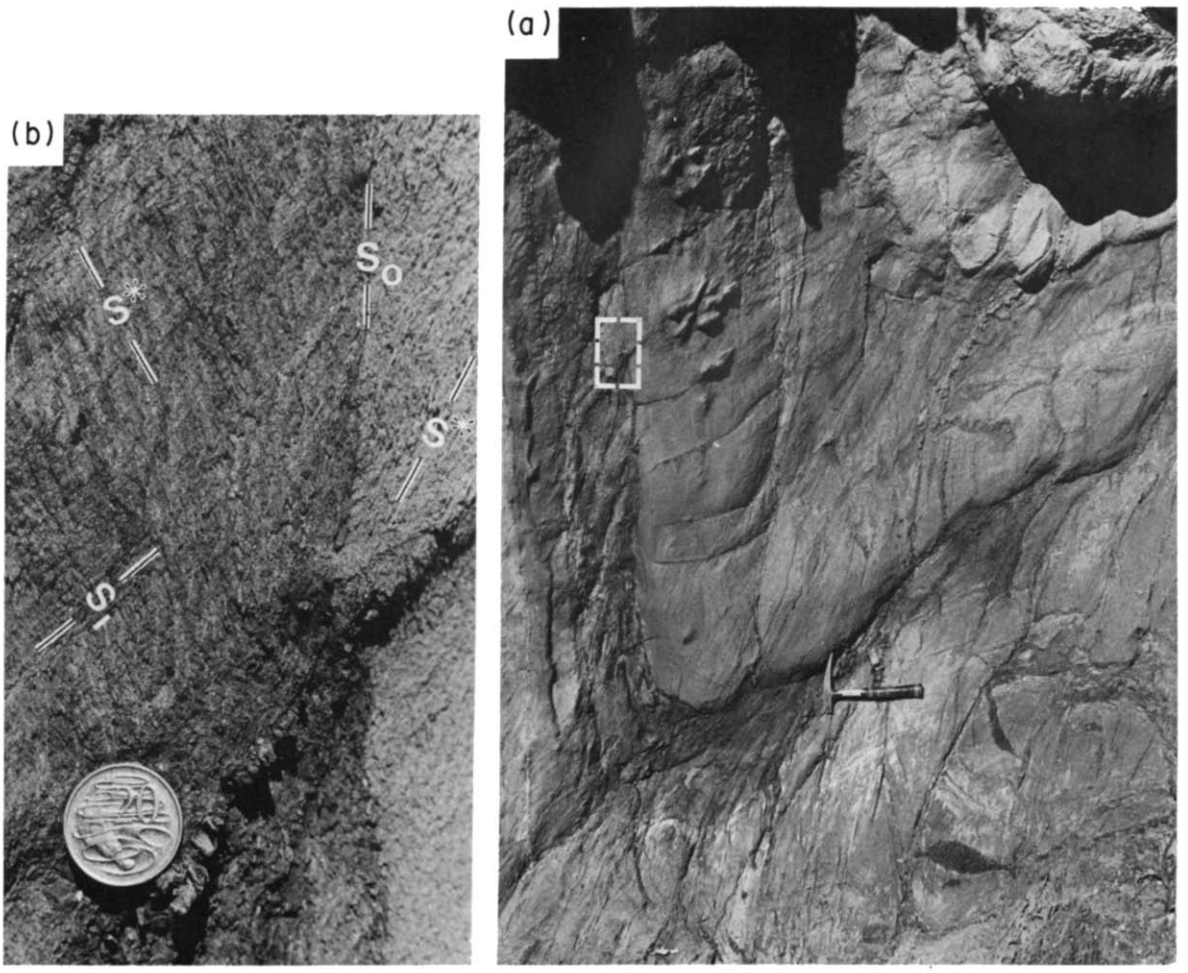

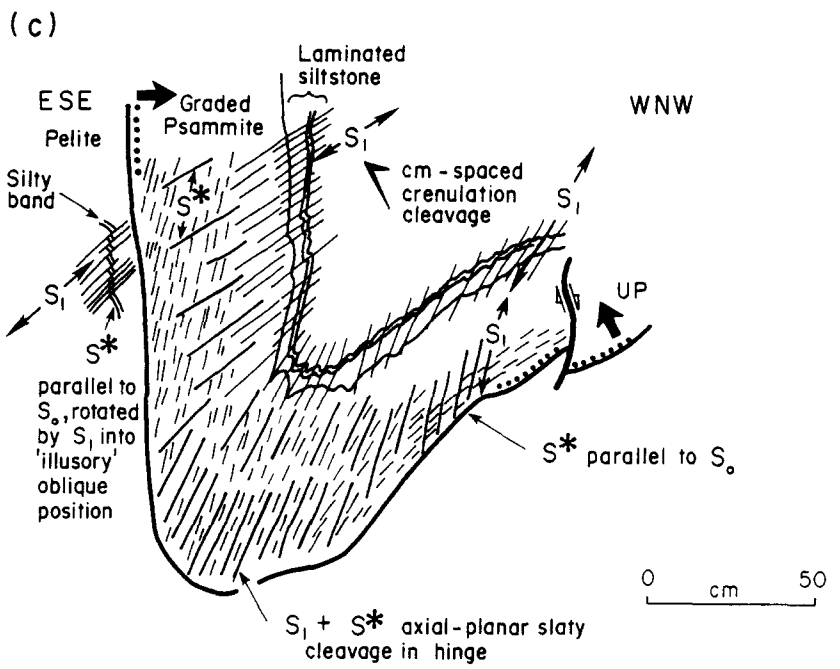

Fig. 10. (a) F_1 fold between 15 and 20 m on Bermagui Headland profile (Fig. 1b). (b) Enlargement of boxed area in (a) showing 'optical illusion' effect in pelite. (c) Sketch explaining structural relationships.

Relationship of quartz veins to S*

Many generations of quartz veins developed during the multi-phase deformation history at Bermagui. In some specimens, quartz veins cut the bedding, and in turn are cut by S^*. One such quartz vein is shown in Fig. 9, in which S_0, S^*, S_1 and the quartz vein can all be seen. In the broad-scale view (Fig. 9a), the quartz vein is seen to lie at a high angle to S_0 in the psammite, with S_1 expressed as discrete bundles of dark cleavage folia spaced 0.5–1 cm apart. The quartz vein is folded with axial surfaces oblique to S_1. A rough cleavage, defined by short, discontinuous traces parallel to the axial surface, is S^*. The quartz vein has been thinned by solution removal along S_1. Figure 9(b) shows the detailed view of the tight folds in the quartz vein, the rough, discontinuous nature of S^* in the psammite, and the discrete bundles of cleavage folia that constitute S_1.

The significance of these observations is that S^* shows good evidence of having developed, or continued to develop after the rocks were consolidated sufficiently for quartz veins to form. Moreover, there is evidence of considerable shortening perpendicular to S^*, as shown by the fibrous quartz veins (Fig. 5b), and quartz beards, and the tight folds in the quartz veins (Fig. 9).

DISCUSSION

Factors to be accounted for

The observation that S^* is oblique to bedding in places is paramount in interpreting its significance, because it means that one cannot simply attribute its presence to an inherited depositional orientation (Williams 1972). Six more observations are relevant to assessing its origin.

(1) S^* in the psammite commonly makes a very low angle with, or is indistinguishable from, the orientation of S_0 where it is traced to a psammite–pelite boundary. This geometry implies that if there were any larger-scale folds, the outcrops examined are all on the limbs, and these hypothetical folds must be tight, if not isoclinal. Alternatively, S^* may not be related to a folding deformation.

(2) S^* and S_1 commonly both show congruous vergence with respect to F_1 folds, though in other places S^* is folded by F_1 folds.

(3) Where S^* is folded on the overturned western limbs of large F_1 anticlines near Bermagui, the $S^* \wedge S_0$ vergence indicates an anticline to the east, and is thus congruous with the major F_1 folds.

(4) Downward-facing F_1 structures are absent, apart from local areas clearly related to zones of rotation by F_2 folds.

Observations (1), (3) and (4) indicate that if any large-scale tight or isoclinal folds exist with S^* as an axial-plane structure, then we have sampled only the upright limbs. Moreover, since our mapping and that of Powell *et al.* (1985) and Wilson *et al.* (1982) has extended for over 250 km up and down the southeastern Australian coast without finding any downward-facing F_1 folds not related to F_2 rotation zones, we suggest that there are none. The only possible F^* folds are small isoclines in early quartz veins and minor folds in some pelite layers (e.g. just south of Zane Grey Pool).

(5) The morphology of S^*, especially in siltstones, is that of a strongly developed grain alignment which, in other terranes, might be referred to as a slaty cleavage. In the psammite beds, some of which are coarse to very coarse-grained greywacke, S^* has the morphology of a rough cleavage (Gray 1978, 1982). In the pelite beds, S^* appears as a regularly spaced microbanding, which reflects alternating quartzose and pelitic differentiated layers. S^* here is a segregated cleavage crenulating a fine bedding-parallel lamination.

(6) The evidence of quartz veins post-dating S_0, and being in turn cut by S^*, indicates that the rocks were sufficiently consolidated prior to the development of S^* for brittle fractures to develop and fill with quartz. Although Williams (1972) thought the bedding-parallel foliation was primarily of depositional orientation, he suggested that it may have been enhanced by low-grade metamorphism. He also noted that micaceous partings morphologically indistinguishable from axial-surface foliations occur parallel to bedding in the Bouma *A* division of graded beds, an observation we confirm. However, Bouma *A* units are massive in undeformed turbidites indicating that the bedding-parallel foliation is of post-depositional origin. We think that most, if not all, of the character of S^* developed after sedimentation, in response to tectonic movement.

Implication of S* *being a tectonic foliation*

The recognition that S^* is not simply an enhanced depositional grain alignment throws new light on the status of the younger S_1 cleavage, which is axial surface to the earliest recognisable mesoscopic folds. The morphology of S_1, described in great detail by Williams (1972), is unusual for axial-surface cleavage of first-generation folds in most other parts of the world. Such cleavages are generally slaty in the pelite and rough and disjunctive in the psammite (Borradaile *et al.* 1982). We do not dispute that crenulation cleavage can form parallel to the axial surface of first-generation folds (e.g. Rickard 1961, White & Knipe 1978, Powell *et al.* 1982), but these examples are not nearly as strongly differentiated as S_1 at Bermagui.

Possible reasons why S* *is oblique to* S_0 *and* S_1 *and yet in some places has congruous vergence relationships to* F_1 *folds*

If S^* is not related to an independent, early phase of folding, and S_1 is not an entirely later superposed cleavage, there are two possible explanations of why S^* has a different orientation from S_0 and S_1 and yet has congruous vergence relationships to F_1 folds. (1) S^* developed as a foliation nearly parallel to bedding before F_1 and

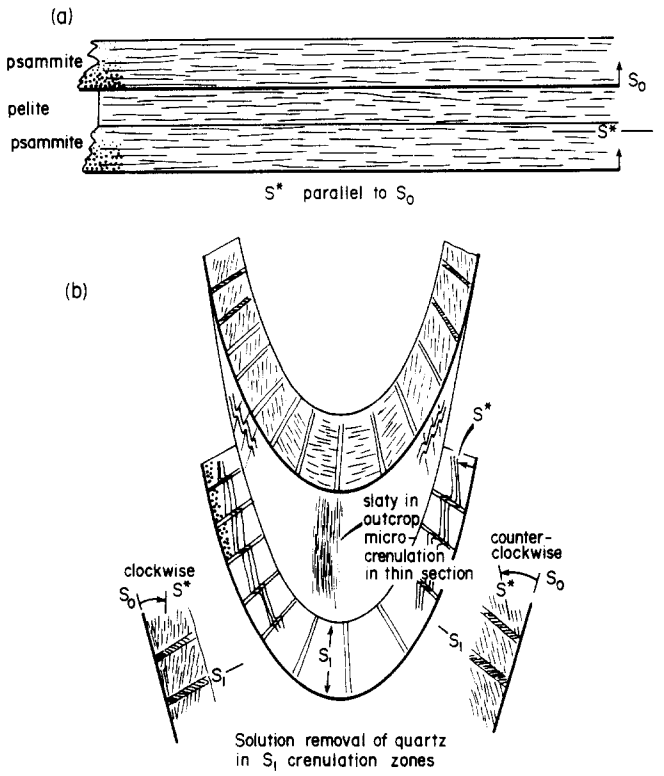

Fig. 11. Model accounting for development of two cleavage surfaces with vergence congruous to minor folds during one deformation. (a) Before folding. (b) After folding. See text for explanation.

was subsequently reoriented by rotation during formation of S_1. The resultant obliquity of S^* to S_0 is more apparent than real and can be attributed to an 'optical-illusion' effect, described below. (2) S^* developed prior to, but in association with, the S_1 cleavage as a protracted response to a single phase of folding, in a manner analogous to that described by Harris *et al.* (1976) and Boulter (1979). These interpretations are not mutually exclusive, and both processes may operate.

(1) *The 'optical-illusion' effect.* Deformation of S_0 and S^* by S_1 commonly produces a scale-dependent 'optical-illusion' effect whereby S^* may appear distinctly oblique to S_0 and S_1, and yet change vergence around an F_1 fold congruously with S_1. The effect is illustrated in Figs. 10 and 11, and is seen in the psammite beds, where S^* lies in the acute angle between S_0 and S_1. This may be explained as follows: prior to F_1 folding, S_0 and S^* were essentially parallel. During F_1 folding, S_1 developed as axial surface to asymmetric crenulation microfolds in S^*, commonly with solution removal of the short limb to give the differentiated cleavage domains so typical of S_1. In the other limb, S^* is inclined to the overall attitude of S_0 (the enveloping surface), and, because of solution removal of material in the S_1 cleavage domains, it is commonly not possible to trace S^* through several S_1 cleavage domains to check whether the enveloping surface to S^* is strictly parallel to S_0. The result is that in outcrop S^* appears inclined to S_0 (Figs. 10b and 11b, enlargements).

The effect can be understood in terms of the fold model in Hobbs *et al.* (1982, fig. 11) where solution removal of most of their β domains (equivalent to S_1) would leave their α domains inclined to the enveloping surface. Some mesoscopic folds that illustrate this phenomenon have been found at Bermagui—the result being that the F_1 fold cores appear to have two cleavages with congruous vergence relationships, or, in the case of the fold at Bermagui Headland (Fig. 10), with opposing vergence in different rock types. The effect is, of course, an optical illusion because where a foliation can be traced through the S_1 cleavage domains, its enveloping surface is seen to be essentially parallel to S_0. Moreover, as the foliation in such folds is traced down-profile towards the base of a sandy layer where S_1 tends to die out, the foliation is seen to become increasingly parallel to S_0. The optical-illusion effect may operate also on foliations at a small angle to bedding (Fig. 10), but in the Bermagui area it cannot explain all the cross-cutting S^* relationships illustrated in this paper.

(2) *Two inclined cleavages during a single folding event.* To the south of Bermagui, F_1 folds are upright, but slightly asymmetric and little affected by F_2 folds and S_2 cleavage. A stripy cleavage (S_1) is common, especially in psammite and laminated pelite, and it fans markedly tending to be parallel to bedding on eastern limbs of anticlines and at a high angle to the axial plane on the western limbs (Rickard 1985). Slaty-type cleavage (S^*) is well-developed in semipelite and pelite, and is axial-planar or tending to divergent fanning. Except in fold hinges, the S^* cleavage consistently lies in the acute angle between the segregation cleavage (S_1) and the bedding. These relationships are similar to those reported by Boulter (1979) for a situation where two inclined cleavages developed during a single folding event. In this case, however, the grain-orientation cleavage (S^*) formed first, and as folding proceeded the segregation cleavage developed by crenulation and solution transfer of the earlier fabric (Fig. 12) (cf. Bradbury & Harris 1982).

A possible sequence of deformation is that if a relatively planar axial-surface foliation, S^*, is acquired as a material surface early in the folding (Fig. 12a), subsequent deformation by intralayer bedding-parallel shear could rotate S^* close to parallelism with S_0 and also set up crenulation–microfold instabilities at a higher angle to S_0 than S^* (Fig. 12b). Continued deformation by bulk flattening and local solution removal of quartz in the crenulation microfolds could have developed S_1 with the characteristic congruous fanning and vergence relationship to the F_1 hinge (Fig. 12c).

Reasons why S* *is locally folded by* F_1 *folds*

There are three possible explanations of why S^* is locally folded around the noses of F_1 folds. The first and favoured explanation is that some minor folds nucleated late during the F_1 folding on the short, straight limbs of early-formed folds after the S^* cleavage had formed as a penetrative axial-surface cleavage. In this model, the late-stage folds would have had to nucleate only on the western limbs of upright F_1 anticlines (Fig. 13).

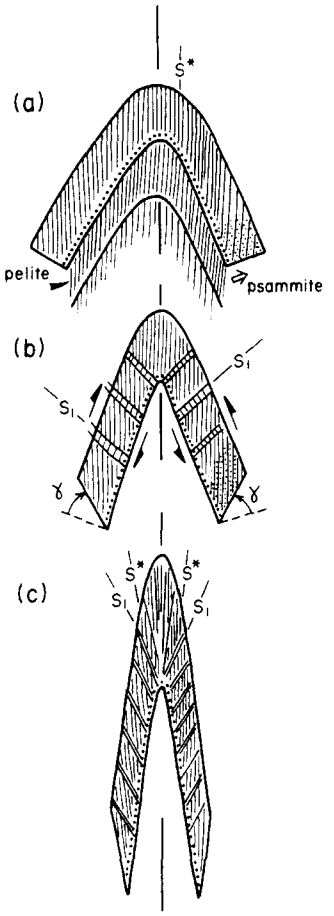

Fig. 12. Model for generation of S^* and S_1 with congruous vergence to F_1 folds during a single protracted folding sequence. (a) Stage at which a penetrative axial-surface foliation, S^* is acquired in all rock types. The foliation may refract from psammite to pelite, but the geometry of subsequent stages is easier to accomplish if the angle between S_0 and S^* is not too high. (b) Continued folding accomplished partly by bedding-parallel simple shear rotating S^* to a low angle with respect to S_0 and nucleating cross-cutting microfold instabilities at a high angle to S_0 (the incipient S_1). (c) Completion of folding with S_1 becoming accentuated by solution-removal of quartz in crenulation microfolds during bulk flattening of the fold profile. S_1 generally fans asymmetrically such that it lies closer to S_0 on eastern limbs of W-facing anticlines.

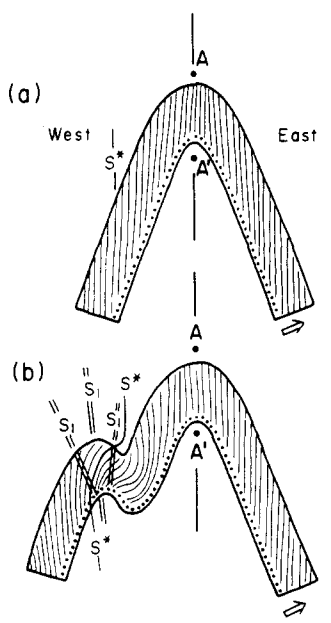

Fig. 13. Late-stage hinge-nucleation model of the occurrence of S^* folded around minor F_1 hinges. (a) Early stage of folding with S^* at a low angle to S_0 on the short straight limb. (b) Wrap-around of S^* by late F_1 hinge.

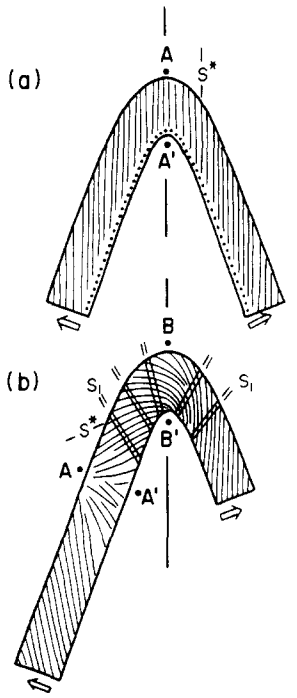

Fig. 14. Hinge-migration model of the occurrence of S^* folded around some minor F_1 hinges. (a) Stage at which S^* is parallel to the fold axial surface and changes vergence congruously around the hinge points A–A'. Arrows indicate sedimentary younging. (b) Migration of the fold hinge wrapping S^* around the minor fold in a refold relationship. S_1 shows congruous vergence with the late-stage axial surface B–B', with the S^* vergence change now on the limb.

The second explanation is that migration of the fold hinge to which S^* was originally axial-planar, folded S^* to produce a wrap-around geometry (Fig. 14). Figures 5 and 7 are possible examples, with the sense of hinge migration being to the east. In the figured examples, hinge migration of a few cm (Fig. 7) to a metre (Fig. 5, also Powell 1983a, fig. 53b) would suffice to explain the observed relationships in outcrop, although we have not found the expected reversal of S^* vergence on the fold limbs signifying the position of the earlier hinge. S^* vergence changes may be present somewhere along the F_1 fold limbs, but have not been found in the exposures available, which permit checking over limb distances generally <2 m.

The third possible explanation is that S^* is in places a genuinely earlier foliation unrelated to F_1. S^* might, for example, be related to early imbricate stacking of the turbidite succession as suggested by Powell (1983a). If S^* is of this origin, then it formed deep in the imbricate wedge because there is no associated chaotic bedding or scaly foliation typical of the shallow regions of accretionary prisms (Carson *et al.* 1982, Moore *et al.* 1982). In this case, the foliation labelled S^* may have a composite origin with some parts of the structure forming before any F_1 folds and other parts (showing congruous vergence relationships to F_1 folds) forming early during F_1.

Timing of deformation

The timing of deformation is constrained only by regional geological relationships (Powell 1983a,b). The

Bermagui turbidites are probably Late Ordovician, although the only fossils found are Late Ordovician graptolites from cherts and black shale that underlie the greywackes (Jenkins *et al.* 1982). S^* can thus be no older than Late Ordovician. The younger age is given by the F_1 folds that deform Late Silurian rocks in the Araluen area (Wyborn & Owen 1979) and are in turn overprinted by contact metamorphism induced by the Early Devonian Bega Batholith. S^* may thus have formed at any time between the deposition of the turbidites and the end of the Silurian.

CONCLUDING REMARKS

Our major conclusion is that at Bermagui there is a well-developed tectonic foliation that pre-dates the differentiated crenulation cleavage, S_1, related to the first-generation of mesoscopic folds. This early foliation, S^*, is oblique to S_0 in many places, and shows various relations to mesoscopic F_1 folds, possibly indicating more than one origin for the S^* foliation. Formation of S^* prior to any F_1 folding, or formation of S^* during F_1 folding with fold-hinge migration and/or late fold-hinge nucleation may all have played a part in determining the geometry of S^*. In addition, there may be some orientation inherited from depositional and diagenetic processes.

The implications of these findings are twofold. First, they open new avenues of interpretation of the S_1 cleavage fabrics described in detail by Williams (1972), and discussed in Hobbs *et al.* (1976). Secondly, they document another example of more than one cleavage possibly related to a single generation of folding (cf. Harris *et al.* 1976, Boulter 1979). The significance of this latter conclusion is that in areas less well exposed, where deformation chronology is commonly built up from relations in isolated outcrops, one might conclude that there was a regional pre-F_1 deformation. However, while this is a possibility, the relations described are equivocal and we must leave the question of a pre-F_1 deformation open.

Acknowledgements—Our interpretation of the early cleavage at Bermagui has developed progressively over several years during field discussions. We thank the many geologists who have participated in these often-animated discussions. Paul Williams suggested the optical illusion effect to M. J. R. Ron Vernon helped improve an early draft and the delegates to Bermagui '84 helped sharpen our appreciation of the many possible models for the S^* cleavage. Field work was funded by our Universities and the Australian Research Grants Scheme.

REFERENCES

Borradaile, G. J., Bayly, M. B. & Powell, C. McA. (editors). 1982. *Atlas of Deformational and Metamorphic Rock Fabrics*. Springer, Heidelberg.

Boulter, C. A. 1979. On the production of two inclined cleavages during a single folding event; Stirling Ranges, S.W. Australia. *J. Struct. Geol.* **1**, 207–220.

Bradbury, H. J. & Harris, A. L. 1982. Low-grade Dalradian sediments carrying spaced cleavage—III. The formation of spaced cleavage. In: *Atlas of Deformational and Metamorphic Rock Fabrics* (edited by Borradaile, G. J., Bayly, M. B. and Powell, C. McA.). Springer, Heidelberg, 104–105.

Carson, B., von Huene, R. & Arthur, M. 1982. Small-scale deformation structures and physical properties related to convergence in Japan trench slope sediments. *Tectonics* **1**, 277–301.

Cole, J. P. 1982. The structure and stratigraphy of the Bodalla area, N.S.W. Unpublished B.Sc. (Hons) thesis, Macquarie University.

Gray, D. R. 1978. Cleavages in psammitic rocks from southeastern Australia: their nature and origin. *Bull. geol. Soc. Am.* **89**, 577–590.

Gray, D. R. 1982. Cleavages in psammitic rocks. In: *Atlas of Deformational and Metamorphic Rocks Fabrics* (edited by Borradaile, G. J., Bayly, M. B. & Powell, C. McA.). Springer, Heidelberg, 112–113.

Harris, A. L., Bradbury, H. J. & McGonigal, M. H. 1976. The evolution and transport of the Tay Nappe. *Scott. J. Geol.* **12**, 103–113.

Hobbs, B. E. 1962. Structural analysis of a small area in the Wagonga Beds at Narooma. *J. geol. Soc. Aust.* **9**, 71–86.

Hobbs, B. E., Means, W. D. & Williams, P. F. 1976. *An Outline of Structural Geology*. Wiley, New York.

Hobbs, B. E., Means, W. D. & Williams, P. F. 1982. The relationship between foliation and strain: an experimental investigation. *J. Struct. Geol.* **4**, 411–428.

Jenkins, C. J., Kidd, P. R. & Mills, K. J. 1982. Upper Ordovician graptolites from the Wagonga Beds near Batemans Bay, New South Wales. *J. geol. Soc. Aust.* **29**, 367–373.

Moore, J. C., Biju-Duval, B. *et al.* 1982. Offscraping and underthrusting of sediment at the deformation front of the Barbados Ridge: Deep Sea Drilling Project Leg 78A. *Bull. geol. Soc. Am.* **93**, 1065–1077.

Powell, C. McA. 1983a. Geology of the N.S.W. South Coast and adjacent Victoria with emphasis on the Pre-Permian structural history. *Geol. Soc. Aust. SGTSG Field Guide* **1**, 1–118.

Powell, C. McA. 1983b. Tectonic relationship between the Late Ordovician and Late Silurian palaeogeographies of southeastern Ausralia. *J. geol. Soc. Aust.* **30**, 353–373.

Powell, C. McA., Cole, J. P. & Cudahy, T. J. 1985. Megakinking in the Lachlan Fold Belt. *J. Struct. Geol.* **7**, 281–300.

Powell, C. McA., Morritt, R. F. C. & Vernon, R. H. 1982. Crenulation morphology of a first-generation cleavage. In: *Atlas of Deformational and Metamorphic Rock Fabrics* (edited by Borradaile, G. J., Bayly, M. B. & Powell, C. McA.). Springer, Heidelberg, 164–165.

Rickard, M. J. 1961. A note on cleavages in crenulated rocks. *Geol. Mag.* **98**, 324–332.

Rickard, M. J. 1985. The structure of the coastal Ordovician rocks south of Bermagui, N.S.W. (abstract). *J. Struct. Geol.* **7**, 498.

White, S. H. & Knipe, R. J. 1978. Microstructure and cleavage development in selected slates. *Contr. Miner. Petrol.* **66**, 165–174.

Williams, P. F. 1970. A criticism of the use of style in the study of deformed rocks. *Bull. geol. Soc. Am.* **81**, 3283–3296.

Williams, P. F. 1971. Structural analysis of the Bermagui area, N.S.W. *J. geol. Soc. Aust.* **18**, 215–228.

Williams, P. F. 1972. Development of metamorphic layering and cleavage in low grade metamorphic rocks at Bermagui, Australia. *Am. J. Sci.* **272**, 1–47.

Williams, P. F. 1979. The development of asymmetrical folds in a cross-laminated siltstone. *J. Struct. Geol.* **1**, 19–30.

Williams, P. F. 1982. Differentiated layering. In: *Atlas of Deformational and Metamorphic Rock Fabrics* (edited by Borradaile, G. J., Bayly, M. B. & Powell, C.McA.). Springer, Heidelberg, 526–527.

Wilson, C. J. L. 1968. Geology of the Narooma area, N.S.W. *J. Proc. R. Soc. N.S.W.* **101**, 147–157.

Wilson, C. J. L., Harris, L. B. & Richards, A. L. 1982. Structure of the Mallacoota area, Victoria. *J. geol. Soc. Aust.* **29**, 91–105.

Wyborn, D. & Owen, M. 1979. Araluen excursion. *Rec Bur. Miner. Resourc. Aust.*